Adsorption of Ethylene on Neutral, Anionic, and Cationic Gold Clusters

Andrey Lyalin*,†,§ and Tetsuya Taketsugu†,‡

Division of Chemistry, Graduate School of Science, Hokkaido University, Sapporo 060-0810, Japan, and Department of Theoretical and Computational Molecular Science, Institute for Molecular Science, Okazaki 444-8585, Japan

Received: October 3, 2009; Revised Manuscript Received: December 8, 2009

The adsorption of ethylene molecules on neutral, anionic, and cationic gold clusters consisting of up to 10 atoms has been investigated using density functional theory. It is demonstrated that C_2H_4 can be adsorbed on small gold clusters in two different configurations, corresponding to the π- and di-σ-bonded species. Adsorption in the π-bonded mode dominates over the di-σ mode over all considered cluster sizes n, with the exception of the neutral $C_2H_4-Au_5$ system. A striking difference is found in the size dependence of the adsorption energy of C_2H_4 bonded to the neutral gold clusters in the π and di-σ configurations. The important role of the electronic shell effects in the di-σ mode of ethylene adsorption on neutral gold clusters is demonstrated. It is shown that the interaction of C_2H_4 with small gold clusters strongly depends on their charge. The typical shift in the vibrational frequencies of C_2H_4 adsorbed in the π and the di-σ configurations gives a guidance to experimentally distinguish between the two modes of adsorption.

Introduction

The adsorption of unsaturated hydrocarbons on transition-metal surfaces has been studied extensively in order to understand the nature of hydrocarbon−metal interaction and chemical processes on solid surfaces; see, e.g., refs 1−6 and references therein. The most significant attention was paid to the investigation of ethylene adsorption[7−17] because it is the simplest alkene containing an isolated carbon−carbon double bond. Hence, it can be treated as a prototype to study the interaction and reactivity of different alkenes on metal surfaces. Moreover, the ethylene epoxidation is one of the most important processes in the chemical industry because the product of such a reaction—ethylene oxide—is widely used in various applications; see, e.g., refs 1, 2, and 18−21 and references therein.

Ethylene can adsorb on metal surfaces in two different configurations.[1,11,12,14] The first one is the π mode where one metal atom on the surface is involved in the adsorption of ethylene via a π bonding. The second one is the di-σ-bonded mode, when two metal atoms are involved in the adsorption via a σ bonding. It was found that the di-σ mode of adsorption is characterized by the increasingly important role of sp^3 hybridization in ethylene, whereas sp^2 hybridization (typical for free molecules) remains unchanged for π-bonded species.[11,12,14]

The bonding of ethylene with transition metals involves electron transfer from the filled bonding π orbital of the ethylene to the metal, alongside a back-donation from the d orbital of the transition metal to the empty π^* antibonding orbital of ethylene, in accordance with the Dewar−Chatt−Duncanson model.[22] Thus, the appearance of the sp^3 character of hybridization in the di-σ-bonded ethylene can be explained by the increasing role of the electron back-donation from the metal to the π^* antibonding orbital of ethylene. Hence, the di-σ-bonded ethylene is activated more strongly in comparison with the π-bonded one; thus, it can be more reactive.[11,12] Therefore, an understanding of the specific mechanisms of ethylene adsorption on metal surfaces is important in order to gain a better insight of the catalytic processes and reactivity of adsorbed hydrocarbons.

Surprisingly, not many studies have been devoted to the investigation of ethylene adsorption on metal clusters and nanoparticles, despite the fact that chemical and physical properties of matter at nanoscale are very different from those of the corresponding bulk solids. These properties are often controlled by quantum size effects and significantly depend on the size and structure of atomic clusters.[23]

A remarkable example is gold. It is well-known that gold in its bulk form is a catalytically inactive and inert metal. However, gold at nanoscale manifests extraordinary catalytic activity that increases with a decrease in the cluster size of up to 1−5 nm.[24−27] Moreover, recent studies demonstrate that catalytic activity of gold clusters adsorbed on an iron oxide support correlates with the presence of very small clusters of ∼10 atoms.[28] It was also reported that gold clusters with the number of atoms $n = 3-11$ possess extraordinarily high electrocatalytic activity toward the O_2 reduction reaction in acid solutions.[29] The origin of such size-dependent catalytic activity of gold remains highly debated and has yet to be fully understood. A comprehensive survey of the field can be found in review papers and books; see, e.g., refs 23 and 30−34. It was demonstrated that the catalytic activity of gold clusters depends on the type of the support material, the presence of defects in the material (e.g., F-center defects), the environment, and doping or special additives; see, e.g., refs 25, 31, and 35−38 and references therein. However, experiments indicate that gold clusters deposited on an inert support can efficiently catalyze the process of styrene oxidation by dioxygen.[27] Hence, the origin of catalytic activity derives from the cluster itself, and therefore, even free clusters can be effective catalysts.

Currently, a large variety of catalytic reactions on gold clusters have been studied experimentally. This includes the processes of catalytic oxidation of carbon monoxide, as well

* To whom correspondence should be addressed. E-mail: lyalin@mail.sci.hokudai.ac.jp.
† Hokkaido University.
‡ Institute for Molecular Science.
§ On leave from: Institute of Physics, St. Petersburg State University, 198504 St. Petersburg, Petrodvorez, Russia.

10.1021/jp909505y
Published on Web 01/22/2010

as more complex reactions, such as alcohol oxidation, the direct synthesis of hydrogen peroxide, and alkene epoxidation.[26,27,39,40]

However, theoretical studies of the gold nanocatalysis have mainly focused on the investigation of adsorption and catalytic reaction of O_2 and CO.[31,36] Nonetheless, the theoretical study of the interaction of alkenes with gold clusters has been relatively unexplored, with the exception of works on the binding of propene on gold and mixed gold−silver clusters,[41,42] propene epoxidation,[43] and our work on cooperative adsorption of oxygen and ethylene on gold clusters.[44] In a very recent work, the interaction of ethylene and formaldehyde with small gold clusters Au_n ($n = 1-5$) has been studied.[45]

In this paper, we report the results of a systematic theoretical study of the adsorption of C_2H_4 on free neutral, anionic, and cationic gold clusters consisting of up to 10 atoms. We find that C_2H_4 adsorbs on small gold clusters in two different configurations, corresponding to the π- and di-σ-bonded species. Adsorption in the π-bonded mode dominates over the di-σ mode over all considered cluster sizes, n, with the exception of the neutral $C_2H_4-Au_5$ system, where the di-σ-bonded configuration is energetically more favorable. We find a striking difference in the size dependence of the adsorption energy of C_2H_4 bonded to neutral gold clusters in the π and di-σ configurations. Thus, the adsorption energy of the π-bonded C_2H_4 develops non-monotonically as a function of cluster size with a local minima at $n = 6$. The adsorption energy, calculated for the di-σ-bonded C_2H_4, exhibits pronounced odd−even oscillations, showing the importance of the electronic shell effects in the di-σ mode of ethylene adsorption on gold clusters.

We also demonstrate that the interaction of C_2H_4 with small gold clusters strongly depends on their charge. The excess of a positive or a negative charge on the gold cluster can change the balance between electron donation and back-donation processes. Hence, ethylene adsorption and reactivity can be manipulated by the cluster charge. This effect can be particularly important for understanding the mechanisms of catalytic activation of ethylene adsorbed on small gold clusters.

Theoretical Methods

The calculations are carried out using density functional theory (DFT). The hybrid Becke-type three-parameter exchange density functional paired with the gradient-corrected Perdew−Wang 91 correlation functional (B3PW91)[46] is used. The choice of the B3PW91 functional is consistent with our previous work on cooperative adsorption and catalytic oxidation of ethylene on small gold clusters.[44] The obtained theoretical data on dissociation energies and bonding in Au_2 (1.904 eV, 2.546 Å) and C_2H_4 (7.596 eV, 1.324 Å) are in a good agreement with those of earlier experimental studies, Au_2 (2.30 eV, 2.472 Å)[47] and C_2H_4 (7.76 eV, 1.339 Å).[48] The standard LANL2DZ basis set of primitive Gaussians is used to expand the gold cluster orbitals formed by the $5s^25p^65d^{10}6s^1$ outer electrons of Au (19 electrons per atom). The remaining 60 core electrons of the Au atom are represented by the Hay−Wadt effective core potential accounting for relativistic effects.[49] For carbon and hydrogen, the aug-cc-pVTZ basis set[50] is employed. The single-point counterpoise correction method has been used to calculate the basis set superposition errors (BSSE). The zero-point energy (ZPE) corrections have been analyzed. Calculations have been carried out with the use of the Gaussian 03 code.[51]

The structural properties of neutral, anionic, and cationic gold clusters have been the subject of numerous theoretical investigations; see, e.g., refs 30−32 for a review. In the present work, the cluster geometries have been determined with the use of the cluster fusion algorithm[52] that belongs to the class of genetic global optimization methods.[53,54] We have successfully used a similar approach to find the optimized geometries of various types of atomic clusters.[58−60] Additionally, the global reaction route mapping (GRRM) technique within the scaled hypersphere search (SHS) method has been used in order to find equilibrium structures.[55−57] The optimized structures of the gold clusters Au_n, Au_n^-, and Au_n^+ ($n = 1-10$) obtained in the present work are presented in the Supporting Information to this paper. These structures are in good agreement with those reported in previous theoretical studies; see, e.g., refs 32 and 61−64.

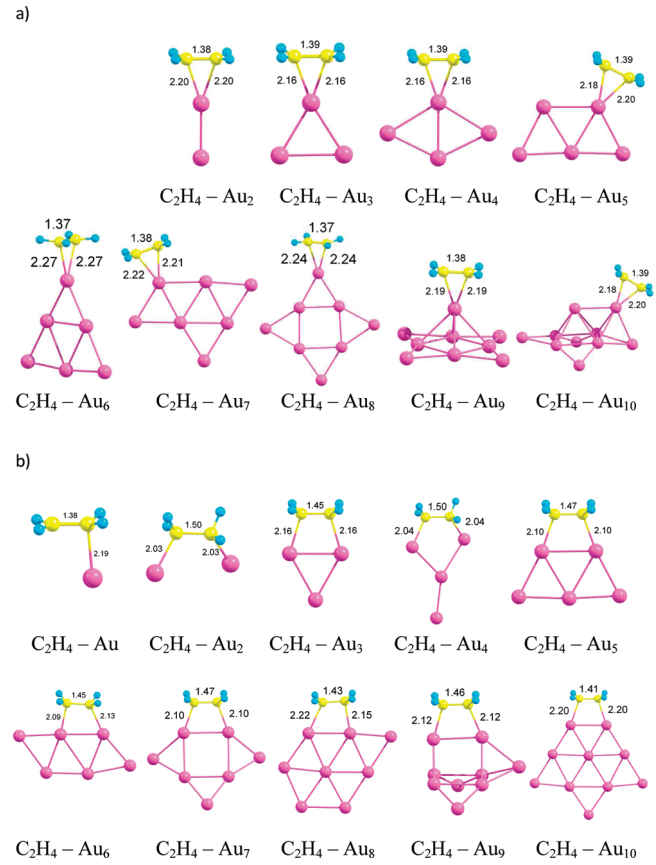

Figure 1. Optimized geometries of neutral $C_2H_4-Au_n$ clusters: (a) π mode of adsorption and (b) di-σ mode of adsorption (in the case of a single Au atom, only one σ bond is formed). The C−C and C−Au interatomic distances are given in angstroms.

To obtain the most stable configuration of C_2H_4 adsorbed on neutral, anionic, and cationic gold clusters, we have created a large number of starting geometries by adding the C_2H_4 molecule in different positions (up to 30) on the surface of the most stable cluster and up to eight isomer structures of the corresponding Au_n, Au_n^-, and Au_n^+ clusters. The starting structures have been optimized further without any geometry constraints.

Theoretical Results

Geometry Optimization for Ethylene Adsorbed on Neutral, Cationic, and Anionic Gold Clusters. The results of the cluster geometry optimization for neutral $C_2H_4-Au_n$, anionic $C_2H_4-Au_n^-$, and cationic $C_2H_4-Au_n^+$ clusters within the size range of $n \leq 10$ are shown in Figures 1−3, respectively.

Gold clusters with adsorbed ethylene possess various isomer forms whose number grows dramatically with cluster size. Among the huge variety of different isomers, one can distinguish two specific adsorption modes that correspond to the π and di-σ

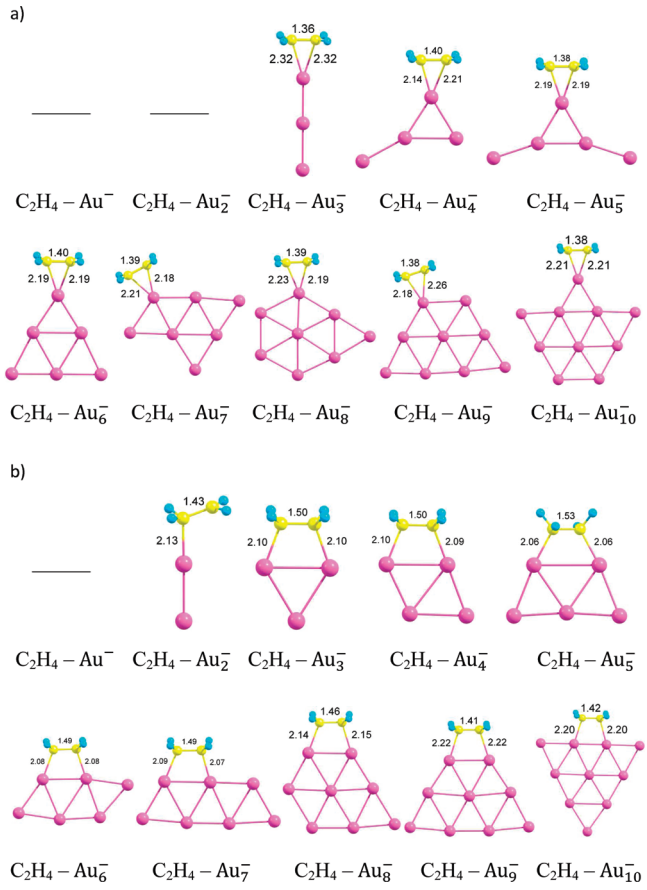

Figure 2. Same as in Figure 1, but for anionic $C_2H_4-Au_n^-$ clusters. In the case of a Au_2^- dimer, only one σ bond is formed.

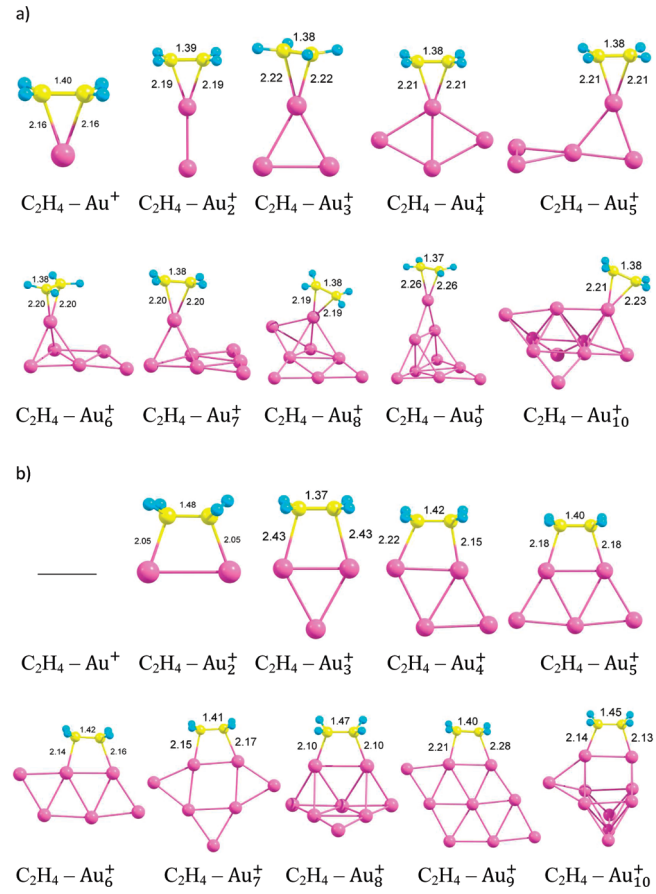

Figure 3. Same as in Figure 1, but for cationic $C_2H_4-Au_n^+$ clusters.

configurations of the adsorbate. The appearance of two different modes of ethylene adsorption on small gold clusters is similar to that reported for ethylene adsorption on Au(100) and Au(111) surfaces.[14] However, in the case of adsorption on the bulk, there are only two possible geometrical configurations of ethylene (we do not consider here μ-bridging species[14] because ethylene adsorption in such a configuration is not possible in the case of small clusters). Moreover, there are no structural changes of the bulk surface due to adsorption of ethylene. In the case of ethylene adsorption on small gold clusters, each of the π and di-σ configurations possesses a variety of structural isomers. These isomers correspond to the adsorption in nonequivalent positions on the surface of clusters. In Figures 1−3, we present the most stable structures of π- and di-σ-bonded ethylene adsorbed on small gold clusters. The C−C and C−Au interatomic distances are given in angstroms.

The interaction of gold clusters with ethylene results in an electron donation from the C_2H_4 to the gold cluster alongside a back-donation from the cluster to the adsorbate, in accordance with the Dewar−Chatt−Duncanson model.[22] The rearrangement of the electronic structure and electron transfers upon adsorption lead to a dramatic change in cluster geometry. The interplay of electronic and geometry shell effects also influences the cluster structure.[60]

Free neutral gold clusters possess planar, two-dimensional (2D) structures when the cluster size is up to 13 Au atoms.[64,65] In the Supporting Information, we present the most stable structures obtained for Au_n, Au_n^+, and Au_n^- clusters ($n = 1-10$) within the B3PW91/LANL2DZ DFT method. Figure 1 demonstrates that the adsorption of C_2H_4 in the π configuration leads to a prevalence of three-dimensional (3D) structures of gold clusters for $n \geq 9$; the structures of small Au_3 and Au_4 clusters transform to those that are energetically favorable for free cations, Au_3^+ and Au_4^+, respectively. For $n < 9$, ethylene favorably adsorbs at the cluster edge where the carbon−carbon bond lies in the plane of the cluster, with the exception of the $C_2H_4-Au_6$ system, where the carbon−carbon bond is located perpendicular to the cluster plane (see Figure 1).

The adsorption of C_2H_4 in the di-σ configuration results in a considerable rearrangement in the structure of neutral gold clusters. Thus, the geometry of Au_3 and Au_6-Au_{10} clusters changes upon C_2H_4 adsorption. It is known that gold clusters possess a large number of energetically close-lying structural isomers.[30,32] Interaction with the adsorbate can easily alter their energy order. It is important to note that interaction with the adsorbate can be responsible for structural rearrangements even for the relatively large clusters. Thus, recent DFT calculations demonstrate that the morphology of the Au_{79} nanoparticle can be transformed by interactions with a CO atmosphere.[66]

It is not surprising that the structures of positively and negatively charged ionic gold clusters change upon ethylene adsorption. Figure 2 demonstrates that, although anionic gold clusters Au_n^- with $n = 1-10$ remain planar upon ethylene adsorption (for both the π and the di-σ adsorption configurations), they manifest considerable structural rearrangements. Thus, gold cluster anions alter their structure upon ethylene adsorption in the π configuration for $n = 4$, 7, 8, and 10. In the case of the di-σ mode of ethylene adsorption, structural rearrangements occur for gold cluster anions with $n = 3-8$. A carbon−carbon bond of the adsorbed ethylene lies in a cluster plane for all structures presented in Figure 2.

Figure 3 shows that, in the case of ethylene adsorption on gold cluster cations, Au_n^+, the resulting cluster systems

TABLE 1: Molecular Adsorption Energies, E_{ads}^{π} and $E_{ads}^{di\text{-}\sigma}$, Calculated for C_2H_4 Adsorbed on the Neutral Au_n Clusters as the π and di-σ Species, Respectively. The Adsorption Energies Modified with Corrections for Zero-Point Vibrational Energy and Basis Set Superposition Errors Are Denoted by $E_{ads,\,ZPE}$ and $E_{ads,\,BSSE}$, Respectively[a]

n	E_{ads}^{π}	$E_{ads,\,ZPE}^{\pi}$	$E_{ads,\,BSSE}^{\pi}$	$E_{ads}^{di\text{-}\sigma}$	$E_{ads,\,ZPE}^{di\text{-}\sigma}$	$E_{ads,\,BSSE}^{di\text{-}\sigma}$
1				0.43	0.41	0.31
2	1.30	1.23	1.17	0.26	0.18	0.07
3	1.59	1.51	1.44	0.95	0.89	0.77
4	1.60	1.51	1.46	0.21	0.13	0.03
5	1.09	1.01	0.96	1.14	1.08	0.97
6	0.80	0.74	0.69	0.07	0.01	−0.09
7	1.03	0.96	0.91	0.79	0.73	0.64
8	0.95	0.88	0.83	0.25	0.19	0.08
9	1.08	1.00	0.93	0.74	0.68	0.56
10	1.06	0.98	0.91	0.42	0.38	0.27

[a] All energies are given in eV.

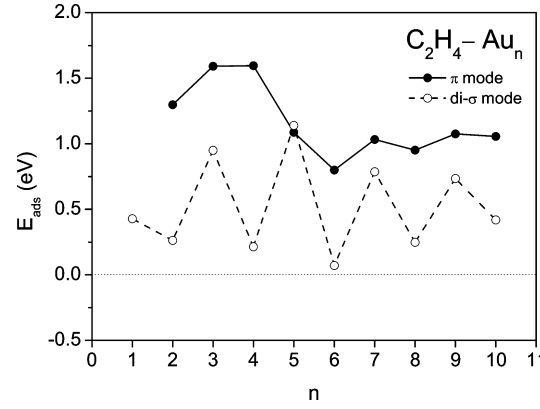

Figure 4. Molecular adsorption energy, E_{ads}, calculated for C_2H_4 adsorbed in π (solid line) and di-σ (dashed line) configurations on the neutral Au clusters with $1 \le n \le 10$. Note that, in the case of a single Au atom, only one σ bond is formed.

$C_2H_4-Au_n^+$ exhibit 3D structures for $n = 5-10$, in the case of the π mode of ethylene adsorption, and $n = 8$ and 10, in the case of the di-σ mode. In both cases of the π and di-σ modes of ethylene adsorption, the structural rearrangements in gold cluster cations occur for $n \ge 5$.

Such a severe change in the morphology of gold clusters due to the interaction with ethylene makes the procedure of structural optimization rather complicated. To get energetically favorable structures of $C_2H_4-Au_n$, $C_2H_4-Au_n^-$, and $C_2H_4-Au_n^+$ clusters, it is necessary to consider the adsorption of ethylene not only on the most stable structures of the corresponding Au_n, Au_n^-, and Au_n^+ clusters but also on a large number of their energetically less favorable isomer states. In the present work, we have taken into account up to eight isomer structures of the host gold clusters. This insures that we do not miss energetically favorable structures with considerable change in cluster geometry due to C_2H_4 adsorption.

Energetics of Ethylene Adsorption on Neutral, Anionic, and Cationic Gold Clusters. We first study the energetics of C_2H_4 adsorption on neutral gold clusters Au_n with $1 \le n \le 10$. The spin states of the optimized $C_2H_4-Au_n$ structures are doublet and singlet for odd and even n, respectively. The adsorption energy is defined as

$$E_{ads} = E_{tot}(Au_n) + E_{tot}(C_2H_4) - E_{tot}(Au_n - C_2H_4) \quad (1)$$

where $E_{tot}(M)$ denotes the total energy of the most stable structure of the molecule (cluster) "M".

Table 1 reports the molecular adsorption energies, E_{ads}^{π} and $E_{ads}^{di\text{-}\sigma}$, calculated for C_2H_4 adsorbed on the neutral Au_n clusters as the π and di-σ species, respectively. The adsorption energies modified with corrections for zero-point vibrational energy ($E_{ads,\,ZPE}$) and basis set superposition errors ($E_{ads,\,BSSE}$) are also listed in Table 1.

It has been shown that the ZPE and BSSE corrections can slightly modify the adsorption energy of O_2 on small binary alloy clusters of gold.[38] In the case of the adsorption of C_2H_4 on gold clusters, the above corrections, in principle, can affect differently the π and di-σ configurations. Therefore, to clarify this effect, we have employed the ZPE and BSSE corrections in the adsorption energy of C_2H_4 on Au_n. We found that the ZPE correction systematically reduces adsorption energy of ethylene on gold clusters by 0.06−0.08 eV, irrespective of adsorbate configuration. The BSSE corrections reduce the ethylene adsorption energy by 0.14−0.17 eV. Although the ZPE and BSSE corrections slightly modify absolute values of the adsorption energy of C_2H_4 bonded to neutral gold clusters, they do not change the general behavior of E_{ads}^{π} and $E_{ads}^{di\text{-}\sigma}$ as a function of cluster size. A similar conclusion on the role of BSSE corrections in the adsorption of ethylene and formaldehyde on small gold clusters has been made in ref 45. Therefore, all results reported below are presented without ZPE and BSSE corrections.

Figure 4 shows the evolution of the molecular adsorption energy, E_{ads}, calculated for the most bound π and di-σ configurations of adsorbed C_2H_4 as a function of cluster size n.

In our previous work, we have studied the adsorption of ethylene on small neutral gold clusters in the π-bonded configuration.[44] Here, we demonstrate that C_2H_4 can be adsorbed on small gold clusters in two different configurations, corresponding to the π- and di-σ-bonded species. Figure 4 shows that the π-bonded mode of C_2H_4 adsorption is energetically favorable in the considered range of cluster sizes n, with the exception of a single Au atom that interacts with one carbon atom in C_2H_4, forming a σ bond, and the Au_5 cluster, where the di-σ-bonded configuration of $C_2H_4-Au_n$ is 0.05 eV more bounded compared with the π-bonded one. A similar behavior of E_{ads}^{π} and $E_{ads}^{di\text{-}\sigma}$ as a function of cluster size has been reported recently for small gold clusters consisting up to 5 atoms.[45]

It is seen from Figure 4 that the adsorption energy of the π-bonded C_2H_4 on Au_n clusters exhibits a maximum at $n = 3$ and 4, followed by a fast drop with a minimum at $n = 6$. For $6 \le n \le 10$, the adsorption energy of π-bonded C_2H_4 shows a weak oscillatory behavior as a function of n.

The n evolution of the adsorption energy calculated for the di-σ-bonded C_2H_4 is considerably different from that of the π-bonded C_2H_4. Figure 4 demonstrates that the adsorption energy of the di-σ-bonded C_2H_4 has an odd−even oscillatory behavior with a local maxima for odd numbers of Au atoms at $n = 3$, 5, 7, and 9. For clusters with an even number of n, the adsorption energy E_{ads} of the di-σ-bonded C_2H_4 is small. Hence, C_2H_4 readily adsorbs in the di-σ configuration—but only for neutral gold clusters with an odd number of Au atoms.

It is interesting to note that, in the case of C_2H_4 adsorption on a Au(111) surface, the di-σ mode ($E_{ads}^{di\text{-}\sigma} = 0.6502$ eV) is energetically more favorable in comparison with the π mode ($E_{ads}^{\pi} = 0.1545$ eV).[14] A similar effect is observed for C_2H_4 adsorbed on a Au(100) surface where theoretical values of $E_{ads}^{di\text{-}\sigma} = 0.7790$ eV and $E_{ads}^{\pi} = 0.2456$ eV have been reported.[14] It is known that the type of C_2H_4 bonding depends upon the surface structure. It has been found that the π-bonded mode dominates in the adsorption of low-coordinated atoms and step

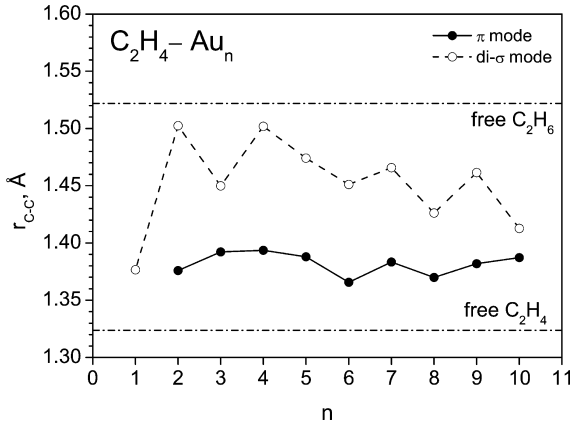

Figure 5. C−C bond distance, r_{C-C}, in C_2H_4 adsorbed in the π (solid line) and di-σ (dashed line) configurations on the neutral Au_n clusters with $1 \leq n \leq 10$. The dashed-dotted lines denote the equilibrium C−C bond distances for free C_2H_4 and C_2H_6. Note that, in the case of a single Au atom, only one σ bond is formed.

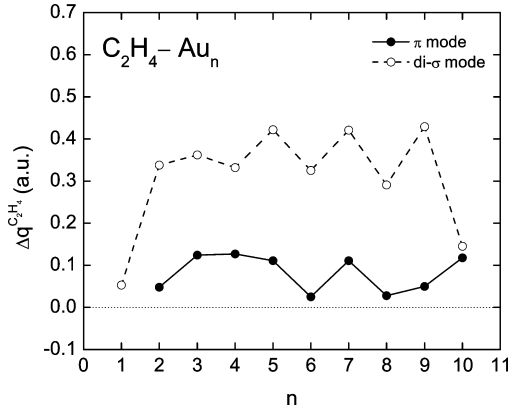

Figure 6. Electron charge transfer, $\Delta q^{C_2H_4}$, to C_2H_4 adsorbed in the π (solid line) and di-σ (dashed line) configurations on the neutral Au clusters with $1 \leq n \leq 10$. Note that, in the case of a single Au atom, only one σ bond is formed.

sites.[67] In the case of small metal clusters, almost all atoms are essentially surface atoms that are undercoordinated as compared with the bulk.[68] Thus, the π-bonded configuration of the adsorbed C_2H_4 dominates for small gold clusters. As the number of low-coordinated atoms decreases with the increase in cluster size, we suppose that the di-σ mode will become dominant for large gold clusters.

Figures 5 and 6 present the n evolution of the C−C bond distance, r_{C-C}, and the total charge transfer to the adsorbate, $\Delta q^{C_2H_4}$, obtained from the natural bond orbitals (NBO) population analysis.[69] Figure 5 shows that the C−C bond in the π-bonded C_2H_4 is enlarged up to 1.37−1.39 Å in comparison with the case of a free C_2H_4 (1.32 Å). The r_{C-C} calculated for the π-bonded C_2H_4 depends slightly on the cluster size, evolving with n similar to E_{ads}. On the other hand, for the di-σ-bonded ethylene, the C−C bond is enlarged up to 1.42−1.50 Å, which is comparable with the length of a single C−C bond in ethane, C_2H_6. The n dependence of r_{C-C} for the di-σ-bonded C_2H_4 manifests an irregular behavior with maxima at $n = 2$, 4, 7, and 9. An increase in the C−C bond length, as well as noticeable change of the bending of the H atoms for di-σ-bonded C_2H_4 (see Figure 1), can be explained by the increasingly important role of the sp^3 hybridization due to the electron donation from the gold cluster to the antibonding π^* orbital of C_2H_4. Therefore, r_{C-C} in the di-σ-bonded ethylene approaches its typical values for a single C−C bond in sp^3-hybridized C_2H_6. Hence, the di-σ-bonded ethylene is activated strongly in comparison with the π-bonded one; thus, it can be more reactive in catalytic processes.

The total charge transfer to the adsorbed C_2H_4 depends on the balance between the donation and back-donation processes. Figure 6 demonstrates that, in the case of the π mode of adsorption, the total charge transfer $\Delta q^{C_2H_4}$ is relatively small and evolves with n similar to r_{C-C}. For the di-σ mode of adsorption, the back-donation from the gold to the π^* antibonding orbital of ethylene dominates over electron transfer from C_2H_4 to the cluster. The total charge transfer to C_2H_4 adsorbed in a di-σ configuration is large and varies in the range of 0.29−0.43 au for $n = 2$−9. It is seen from Figure 6 that $\Delta q^{C_2H_4}$ calculated for the di-σ-bonded C_2H_4 exhibits pronounced odd−even oscillations as a function of cluster size n, with the exception of $n = 1$. Note that, for $n = 1$, the charge transfer $\Delta q^{C_2H_4}$ is small because, in this case, only one Au−C σ bond is formed. Similar odd−even oscillations have been found in the n dependence of the adsorption energy of O_2 on Au_n clusters; see, e.g., refs 23, 61, and 70 and references therein. However, the adsorption energy of CO does not present any odd−even effects.[70]

The appearance of the odd−even oscillations in E_{ads} and $\Delta q^{C_2H_4}$ for the di-σ mode of adsorption is a result of the electronic shell effects[32,71,72] in the gold clusters and can be described within the jellium model. Despite its simplicity, the jellium model can explain, at least on the qualitative level, many physical properties and chemical reactivity of metal clusters.[32,73,74] Indeed, each Au atom has one 6s electron that delocalizes in the whole volume of the cluster. The delocalized electrons are moving in the field of a uniform positive charge background, which binds the valence electron cloud. The gold clusters with an even number of atoms (valence electrons) have a closed electronic shell structure. Hence, these clusters are more stable and less reactive in comparison with open shell clusters possessing an odd number of atoms (valence electrons).

The prevalence of the electron transfer from the cluster to the adsorbate (back-donation process) is responsible for the promotion of the di-σ mode of C_2H_4 adsorption. Indeed, the di-σ mode of C_2H_4 adsorption on small gold clusters with an odd number of atoms leads to the transfer of an unpaired electron from the gold cluster to the ethylene antibonding π^* orbital, causing the weakening of the C−C bond. The neutral gold clusters with an even number of valence electrons possess a closed electronic shell structure; hence, electron transfer to the adsorbate and formation of the di-σ-bonded species is suppressed.

Figure 7 demonstrates the evolution of molecular adsorption energy, E_{ads}, and C−C bond distances, r_{C-C}, as a function of cluster size n for C_2H_4 adsorbed on the anionic Au_n^- (left column) and cationic Au_n^+ (right column) clusters with $1 \leq n \leq 10$.

The adsorption energy of C_2H_4 on a gold cluster depends on the balance between donation and back-donations processes; hence, it can be manipulated by the cluster charge. It is seen from Figure 7a,b that excess of the negative or the positive charges on gold clusters strongly influences the molecular adsorption. Thus, the interaction of C_2H_4 with the negatively charged gold clusters Au_n^- becomes weaker if compared with the neutrals, whereas excess of the positive charge results in strengthening of the C_2H_4 and Au_n^+ bond.

Figure 7a demonstrates that the π mode of C_2H_4 adsorption is not stable for Au^- and Au_2^-. The adsorption energy of the π-bonded C_2H_4 on the gold cluster anions Au_n^- is 0.17 eV, in the case of a trimer Au_3^-, and this increases with an increase

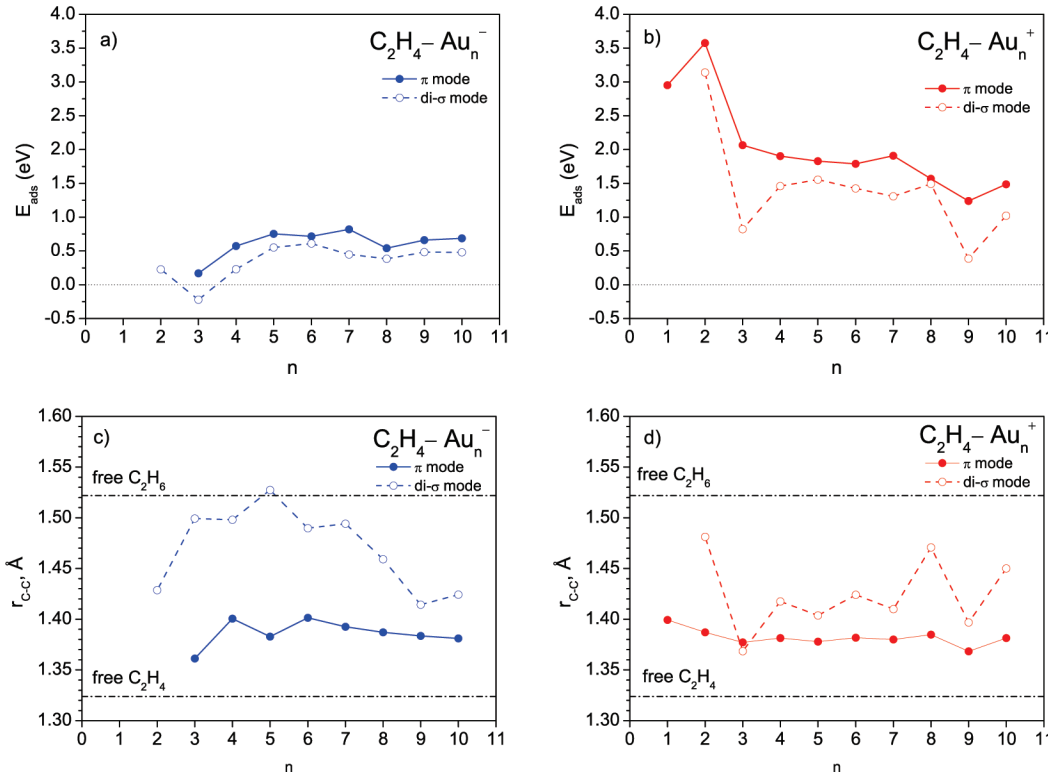

Figure 7. Molecular adsorption energy, E_{ads} (upper row), and C−C bond distances in adsorbed molecules, r_{C-C} (lower row), calculated for C_2H_4 adsorbed on the anionic Au (left column) and cationic Au_n^+ (right column) clusters with $1 \le n \le 10$. Solid and dashed lines correspond to the π and di-σ configurations of adsorbed C_2H_4, respectively. Dashed-dotted lines in the lower row figures denote the equilibrium C−C bond distances for free C_2H_4 and C_2H_6.

in the cluster size: up to 0.82 eV at $n = 7$ and dropping to 0.54 eV at $n = 8$, while slowly increasing with an increase in the cluster size up to $n = 10$.

Figure 7b shows that the size dependence of E_{ads} for π-bonded C_2H_4 on the gold cluster cations Au_n^+ is very different from that of Au_n^-. Thus, C_2H_4 readily adsorbs on the cationic monomer Au^+ and dimer Au_2^+ with an adsorption energy of 2.95 and 3.58 eV, respectively. Further increase in cluster size results in the sharp decrease in E_{ads} up to 2.06 eV for $n = 3$, followed by its slow decrease for $3 \le n \le 6$. At $n = 7$, the adsorption energy E_{ads} exhibits a maximum, followed by the second sharp decrease at $n = 8$ and 9.

For any n in the range of $1 \le n \le 10$, the adsorption energy of the π-bonded C_2H_4 on cationic, $E_{ads}^{\pi}(Au_n^+)$, neutral, $E_{ads}^{\pi}(Au_n)$, and anionic, $E_{ads}^{\pi}(Au_n^-)$, gold clusters satisfies the relation: $E_{ads}^{\pi}(Au_n^+) > E_{ads}^{\pi}(Au_n) > E_{ads}^{\pi}(Au_n^-)$.

Indeed, the excess of the positive charge on the cluster favors the process of electron transfer from the C_2H_4 to the gold cluster, which stabilizes the π mode of adsorption and strengthens the Au−C bond. A similar effect has been found for the adsorption of CO on small anionic and cationic gold clusters.[75,76] It was found that the adsorption energy of CO is larger in the case of a cluster of cations and smaller in the case of anions. With the increasing cluster size, the differences in adsorption energies for different charge states become smaller.[76]

It is important to mention that strengthening the Au−C bond for C_2H_4 adsorbed on the gold clusters with an excess of the positive charge is responsible for a cooperative effect in the simultaneous adsorption of C_2H_4 and O_2 on neutral gold clusters.[44] Indeed, the adsorption of O_2 on Au_n results in an electron transfer from the gold cluster to the antibonding $2\pi^*$ orbital of O_2. In this case, C_2H_4 effectively adsorbs on the positively charged gold cluster. A similar effect has also been predicted for the adsorption of propene on O_2-Au_n clusters.[41] It was supposed that the binding of propene to O_2-Au_n should be stronger than the binding to the Au_n cluster due to the effective charge transfer from the gold cluster to the oxygen molecule.[41]

The excess of the positive or the negative charge on gold clusters results in a considerable change in the adsorption energy of the di-σ-bonded C_2H_4. As has been discussed above, the adsorption energy of the di-σ-bonded C_2H_4 on small neutral gold clusters exhibits odd−even oscillations as a function of the cluster size. These oscillations appear as a result of the electronic shell effects in gold clusters: Au_n with an odd n have one uncoupled electron that can easily transfer to the empty π^* antibonding orbital of C_2H_4. Such an electron transfer favors the di-σ configuration of the adsorbed C_2H_4.

Figure 7a demonstrates that there is no odd−even oscillation in the adsorption energy of the di-σ-bonded C_2H_4 on the anionic Au_n^- clusters. In that case, the cluster always possesses a weakly bounded electron that it can transfer to the adsorbate.

In the case of the cationic Au_n^+ clusters, the electron back-donation process to C_2H_4 is suppressed for any n. Figure 7b shows that E_{ads} calculated for the di-σ-bonded C_2H_4 on Au_n^+ exhibits two profound minima at $n = 3$ and 9. In accordance with the spherical jellium model, Au_3^+ and Au_9^+ clusters possess a closed shell electronic structure with two and eight valence electrons, respectively. Hence, Au_3^+ and Au_9^+ are chemically inactive, in particular, in the processes where electron transfer from the cluster to the adsorbate is responsible for formation of the chemical bond.

Figure 7c,d demonstrates the n evolution of the C−C bond distance, r_{C-C}, in C_2H_4 adsorbed on Au_n^- and Au_n^+ clusters, respectively. The C−C bond in the π-bonded C_2H_4 on the anionic and the cationic clusters is enlarged up to 1.36−1.40

TABLE 2: Vibrational Frequencies of C_2H_4

mode	calculation, cm^{-1}	experiment,[77] cm^{-1}
ν_1 (b_{2u})	826	826
ν_2 (b_{3u})	975	943
ν_3 (b_{2g})	981	949
ν_4 (a_u)	1057	1023
ν_5 (b_{3g})	1237	1236
ν_6 (a_g)	1377	1342
ν_7 (b_{1u})	1467	1444
ν_8 (a_g)	1693	1623
ν_9 (b_{1u})	3131	2989
ν_{10} (a_g)	3146	3026
ν_{11} (b_{3g})	3205	3103
ν_{12} (b_{2u})	3233	3106

Å, irrespective to cluster charge. This is 0.04−0.08 Å larger than that for the free C_2H_4 (1.32 Å). The di-σ-bonded ethylene is activated strongly in the case of adsorption on the anionic Au_n^- clusters. Thus, in the di-σ-bonded ethylene, the C−C bond is enlarged up to 1.53−1.42 Å for the anionic and only up to 1.48−1.37 Å for the cationic gold clusters. Such an effect has a clear explanation. The excess of electrons on a cluster promotes back-donation of an electron from the cluster to the π^* antibonding orbital of C_2H_4, hence promoting its activation. The excess of the positive charge on a cluster suppresses the back-donation process, thereby suppressing the C_2H_4 activation. Thus, by changing the cluster charge, one can manipulate the cluster reactivity.

Vibrational Spectra of Ethylene Adsorbed on Small Gold Clusters. Analysis of the vibrational spectrum of adsorbed C_2H_4 directly reveals the mode of C_2H_4 adsorption and the state of hybridization. This is due to the sensitivity of the C−C stretching frequency to the hybridized state of carbon atoms.[11] In 1985, Stuve and Madix introduced the so-called $\pi\sigma$ parameter for characterizing rehybridization in C_2H_4 upon adsorption on metal surfaces.[11] The $\pi\sigma$ parameter depends on the shift of the C−C stretching frequencies in C_2H_4 and ranges from 0 for the free C_2H_4, to 0.38 for $K[(C_2H_4)PtCl_3]$ (Zeise's salt), and finally to 1 for $C_2H_4Br_2$. Zeise's salt and $C_2H_4Br_2$ have been chosen by Stuve and Madix as models describing pure π and di-σ bonding of C_2H_4, respectively. Thus, the larger the shift in vibrational frequencies (compared to the free C_2H_4), the greater the degree of rehybridization.

A similar approach can be applied for C_2H_4 adsorbed on metal clusters. Table 2 presents the vibrational frequencies of free C_2H_4 calculated in the harmonic approximation and obtained from experiment.[77]

The obtained theoretical results are in a good agreement with experimental data. Some discrepancy, especially noticeable in the high-frequency range, might result from anharmonic effects. The anharmonic corrections can be taken into account, for example, by the vibrational self-consistent field method based on the quartic force field.[78] However, such a consideration goes far beyond the scope of the present paper. To distinguish between π and di-σ modes of C_2H_4 adsorption, one should calculate the shift in the C−C stretching frequencies of the adsorbed C_2H_4 with respect to the free molecule. In that case, the anharmonic corrections to the vibrational energy levels can be partly canceled. Therefore, in this paper, we perform an analysis of the vibrational spectra of the adsorbed C_2H_4 in the harmonic approximation.

Following ref 11, we have selected two vibrational modes: ν_6 and ν_8, corresponding to the direct C−C and the in-plane CH_2 scissoring modes of vibrations, respectively. Information on the shift of the vibrational frequencies of C_2H_4 upon its adsorption can be obtained from infrared or Raman spectroscopy. Figure 8 presents the frequency dependence of the Raman scattering activity calculated for a C_2H_4 molecule adsorbed in the π (Figure 8a) and di-σ (Figure 8b) configurations on the neutral Au_n clusters with $n = 1-10$. The stretching modes corresponding to the ν_6 and ν_8 vibrations in C_2H_4 are marked by the vertical arrows. It is seen from Figure 8a that the spectral dependences of the Raman scattering activity calculated for the π-bonded ethylene on Au_n clusters are similar for all the cluster sizes n considered. The first maximum at 960 cm^{-1} corresponds to the symmetric and asymmetric swinging of H atoms in the direction perpendicular to the plane of C_2H_4—similar to the ν_2 and ν_3 vibrational modes in free C_2H_4. These vibrations remain unchanged in the π-bonded C_2H_4. Two intensive maxima at 1280 and 1560 cm^{-1} correspond to the ν_6 and ν_8 vibrational modes in C_2H_4. These lines are red shifted in comparison with the free C_2H_4.

Solid lines in Figure 9 demonstrate shifts $\Delta\nu_6^{\pi}$ and $\Delta\nu_8^{\pi}$ in harmonic frequencies ν_6 and ν_8 due to the π mode of C_2H_4 adsorption on small neutral gold clusters. For the π-bonded C_2H_4, the scissoring mode ν_8 is shifted by 30−40 cm^{-1} toward low frequencies if compared with the ν_6 mode. Both the $\Delta\nu_6^{\pi}$ and the $\Delta\nu_8^{\pi}$ shifts vary in the range of 58−142 cm^{-1} and exhibit a similar dependence on the cluster size with local minima at $n = 6$ and 8. The relatively small frequency shifts, $\Delta\nu_6^{\pi}$ and $\Delta\nu_8^{\pi}$, correspond to the values of the $\pi\sigma$ parameter typical for the π-bonded C_2H_4.

Figure 8 demonstrates that the spectral behavior of the Raman scattering activity calculated for the di-σ-bonded C_2H_4 is different from that obtained for the π-bonded C_2H_4. Thus, for cluster sizes $n = 2$, 4, 5, 7, and 9, a broad band appears in the frequency region of 900−1300 cm^{-1}. This band results from the strong mixing of the C−C stretching mode ν_6 with the hydrogen swinging (ν_2 and ν_3) and twisting (ν_4) modes. The coupling of the ν_2, ν_3, ν_4, and ν_6 vibrational modes occurs as a result of considerable deformations in C_2H_4. These deformations include the bending of H atoms with respect to the plane of a free C_2H_4 due to the sp^3 hybridization in di-σ-bonded C_2H_4, as well as the twisting of CH_2 groups with respect to each other along the C−C bond. Such twisting is especially noticeable for $C_2H_4-Au_2$ and $C_2H_4-Au_4$ clusters. The strong coupling between different vibrational modes makes identification of ν_6 and ν_8 vibrations rather difficult: the mixed modes form new levels, neither of which represents the true ν_6 and ν_8 states.

The appearance of the sp^3 hybridization character in di-σ-bonded C_2H_4 results in a considerable red shift in the stretching frequencies. Such shifts, $\Delta\nu_6^{\text{di-}\sigma}$ and $\Delta\nu_8^{\text{di-}\sigma}$, in harmonic frequencies ν_6 and ν_8 are shown by the dashed lines in Figure 9.

It is seen that the $\Delta\nu_6^{\text{di-}\sigma}$ shift is considerably larger than the $\Delta\nu_8^{\text{di-}\sigma}$, which can be explained by the strong coupling between the ν_2, ν_3, ν_4, and ν_6 vibrational levels. The $\Delta\nu_6^{\text{di-}\sigma}$ and $\Delta\nu_8^{\text{di-}\sigma}$ frequency shifts vary in the range of 200−370 cm^{-1} for $n = 2-10$. These values correspond to the $\pi\sigma$ parameter typical for the di-σ-bonded C_2H_4. Thus, the analysis of the vibrational modes of C_2H_4 adsorbed on gold clusters allows one to identify the specific modes of C_2H_4 adsorption and the rate of rehybridization upon adsorption.

Conclusions

In summary, we have demonstrated that C_2H_4 can be adsorbed on small gold clusters in two different configurations, corresponding to the π- and di-σ-bonded species. Adsorption in the π-bonded mode dominates over the di-σ mode over all considered cluster sizes n, with the exception of the neutral

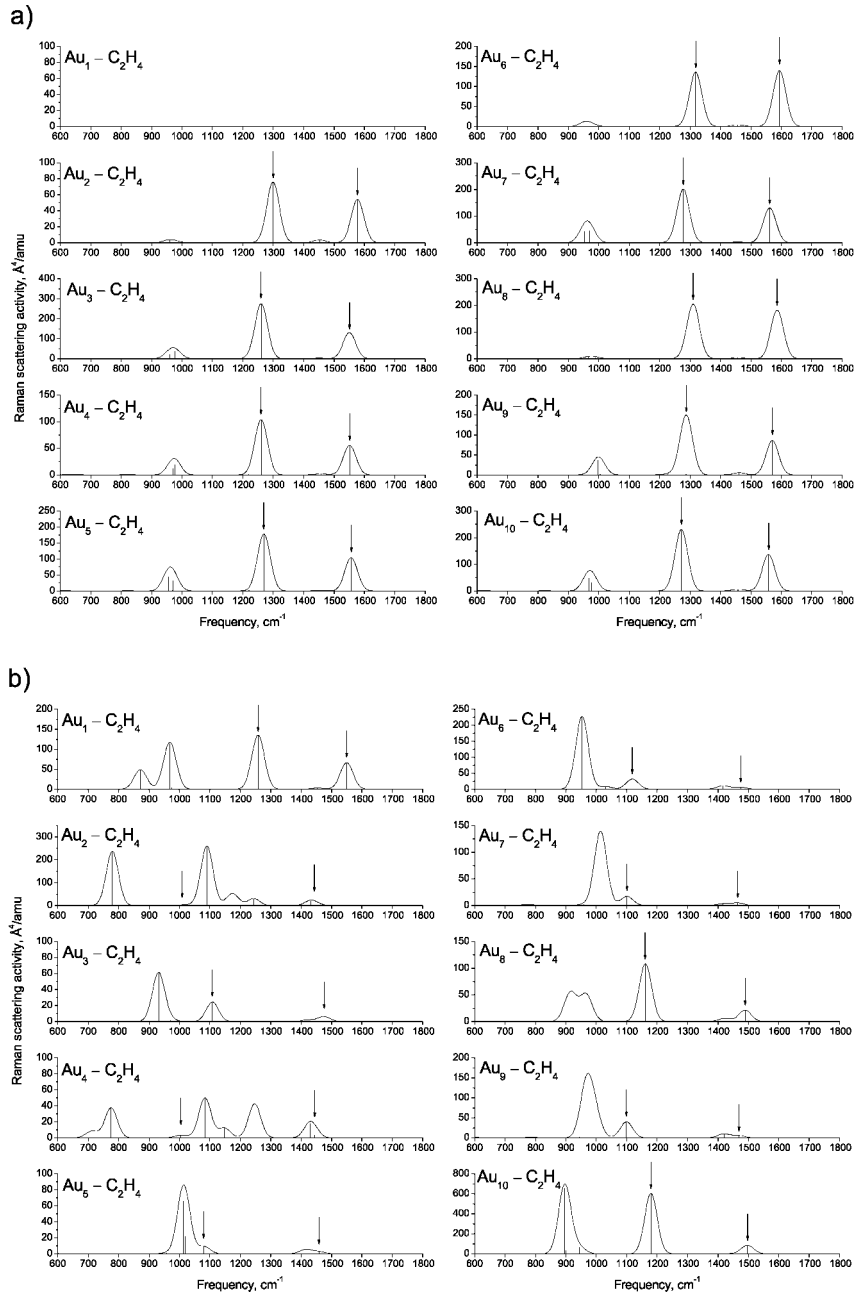

Figure 8. Raman scattering activity of the neutral $C_2H_4-Au_n$ clusters: (a) π-bonded C_2H_4 and (b) di-σ-bonded C_2H_4. Gaussian broadening of half-width 45 cm^{-1} has been used. The stretching modes corresponding to the ν_6 and ν_8 vibrations in C_2H_4 are marked by the vertical arrows. Note that, in the case of a single Au atom, only one σ bond is formed.

$C_2H_4-Au_5$ system. We found a striking difference in the size dependence of the adsorption energy of C_2H_4 bonded to neutral gold clusters in the π and di-σ configurations. The adsorption energy, calculated for the di-σ-bonded C_2H_4, exhibits pronounced odd−even oscillations, showing the importance of the electronic shell effects in the di-σ mode of ethylene adsorption on gold clusters. The different rates of hybridization in the π- and di-σ-bonded C_2H_4 can be responsible for the different rates of catalytic activation and, hence, different reactivities of adsorbed C_2H_4.

We have also demonstrated that the interaction of C_2H_4 with small gold clusters strongly depends on the cluster charge. Hence, ethylene adsorption and reactivity can be manipulated by the cluster charge. The strengthening of the ethylene−cluster interaction for gold clusters with an excess of the positive charge is responsible for the cooperative effect in the simultaneous adsorption of C_2H_4 and O_2 on neutral gold clusters. This effect can play an important role in the mechanism of catalytic oxidation of alkenes by dioxygen on the surface of gold clusters.

Finally, we have shown that the analysis of the vibrational modes of C_2H_4 adsorbed on gold clusters allows one to identify the specific modes of C_2H_4 adsorption, the rate of rehybridization upon adsorption, and thus the C_2H_4 reactivity.

In the present work, we have considered the adsorption of ethylene molecules onto small gold clusters consisting of up to 10 atoms. Many interesting problems beyond the scope of the present work arise when considering multiple molecular adsorptions on gold nanoparticles with larger sizes up to 1−5 nm, where the strong dependence of the catalytic activity of gold nanoparticles has been observed experimentally. In particular, multiple molecular adsorptions on the surface of gold nanopar-

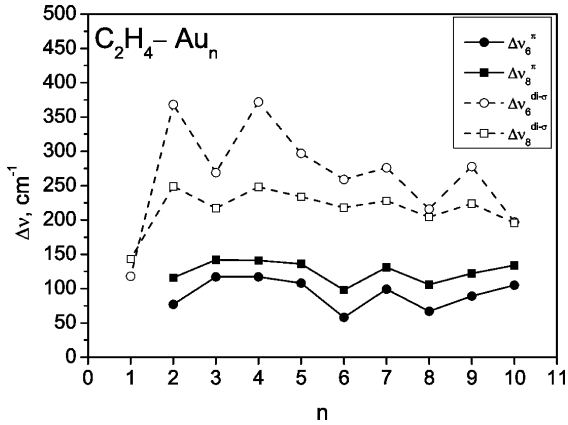

Figure 9. Shift in the harmonic frequencies, ν_6 and ν_8, calculated for the π (solid lines) and di-σ (dashed lines) configurations of adsorbed C_2H_4 on the neutral Au clusters with $1 \leq n \leq 10$. Note that, in the case of a single Au atom, only one σ bond is formed.

ticles can result in a considerable change in cluster morphology, even for relatively large cluster sizes.

Another important direction for future development is to investigate the effect of alloying on the adsorption and catalytic activation of alkenes on gold clusters. The doping of a gold cluster with an atomic impurity can result in considerable changes in the geometrical and electronic structure of the cluster, thereby modifying and controlling the catalytic activity. Understanding how to enhance and control chemical reactions on a cluster surface is, therefore, a vital task for nanocatalysis.

Acknowledgment. This work was supported by the Global COE Program (Project No. B01, Catalysis as the Basis for Innovation in Materials Science) from the Ministry of Education, Culture, Sports, Science and Technology, Japan, and by the Grant-in-Aid for the Project on Strategic Utilization of Elements. The computations were performed using the Research Center for Computational Science, Okazaki, Japan.

Supporting Information Available: Figure of the optimized structures of the most stable neutral, anionic, and cationic gold clusters calculated within the size range of $1 \leq n \leq 10$ in the B3PW91/LanL2DZ approximation. This material is available free of charge via the Internet at http://pubs.acs.org.

References and Notes

(1) Astruc, D. *Organometallic Chemistry and Catalysis*; Springer-Verlag: Berlin, Germany, 2007.
(2) Masel, R. I. *Principles of Adsorption and Reaction on Solid Surfaces*; John Wiley and Sons: New York, 1996.
(3) Sheppard, N.; De La Cruz, C. *Adv. Catal.* **1996**, *41*, 1.
(4) Sheppard, N.; De La Cruz, C. *Adv. Catal.* **1998**, *42*, 181.
(5) Zaera, F. *Chem. Rev.* **1995**, *95*, 2651.
(6) Mrozek, M. F.; Weaver, M. J. *J. Phys. Chem. B* **2001**, *105*, 8931.
(7) Baerends, E. J.; Ellis, D. E.; Ros, P. *Theor. Chim. Acta* **1972**, *27*, 339.
(8) Paulus, U. A.; Wang, Y.; Bonzel, H. P.; Jacobi, K.; Ertl, G. *J. Phys. Chem. B* **2005**, *109*, 2139.
(9) Calaza, F.; Gao, F.; Li, Z.; Tysoe, W. T. *Surf. Sci.* **2007**, *601*, 714.
(10) Watwe, R. M.; Cortright, R. D.; Mavrikakis, M.; Nørskov, J. K.; Dumesic, J. A. *J. Chem. Phys.* **2001**, *114*, 4663.
(11) Stuve, E. M.; Madix, R. J. *J. Phys. Chem.* **1985**, *89*, 3183.
(12) Stuve, E. M.; Madix, R. J. *J. Phys. Chem.* **1985**, *89*, 105.
(13) Cassuto, A.; Mane, M.; Hugenschmidt, M.; Dolle, P.; Jupille, J. *Surf. Sci.* **1990**, *237*, 63.
(14) Zinola, C. F.; Castro Luna, A. M. *J. Electroanal. Chem.* **1998**, *456*, 37.
(15) Ge, Q.; King, D. A. *J. Chem. Phys.* **1999**, *110*, 4699.
(16) Itoh, K.; Kiyohara, T.; Shinohara, H.; Ohe, C.; Kawamura, Y.; Nakai, H. *J. Phys. Chem. B* **2002**, *106*, 10714.
(17) Kokalj, A.; Corso, A. D.; Gironcoli, S.; Baroni, S. *J. Phys. Chem. B* **2006**, *110*, 367.
(18) van Santen, R. A.; Kuipers, H. P. C. E. *Adv. Catal.* **1987**, *35*, 265.
(19) Barteau, M. A.; Madix, R. J. The Surface Reactivity of Silver: Oxidation Reactions. In *The Chemical Physics of Solid Surfaces and Heterogeneous Catalysis*; King, D. A., Woodruff, D. P., Eds.; Elsevier: New York, 1982; Vol. 4.
(20) Torres, D.; Lopez, N.; Illas, F.; Lambert, R. M. *J. Am. Chem. Soc.* **2005**, *127*, 10774.
(21) Torres, D.; Illas, F. *J. Phys. Chem. B* **2006**, *110*, 13310.
(22) Chatt, J.; Duncanson, L. A. J. *J. Chem. Soc.* **1953**, 2939.
(23) Heiz, U.; Landman, U. *Nanocatalysis*; Springer: Berlin, Germany, 2007.
(24) Haruta, M.; Kobayashi, T.; Sano, H.; Yamada, N. *Chem. Lett.* **1987**, *16*, 405.
(25) Haruta, M. *Catal. Today* **1997**, *36*, 2153.
(26) Tsunoyama, H.; Sakurai, H.; Negishi, Y.; Tsukuda, T. *J. Am. Chem. Soc.* **2005**, *127*, 9374.
(27) Turner, M.; Golovko, V. B.; Vaughan, O. P. H.; Abdulkin, P.; Berenguer-Murcia, A.; Tikhov, M. S.; Johnson, B. F. G.; Lambert, R. M. *Nature* **2008**, *454*, 981.
(28) Herzing, A. A.; Kiely, Ch. J.; Carley, A. F.; Landon, P.; Hutchings, G. J. *Science* **2008**, *321*, 1331.
(29) Rodríguez-Vázquez, M. J.; Blanco, M. C.; Lourido, R.; Vázquez-Vázquez, C.; Pastor, E.; Planes, G. A.; Rivas, J.; López-Quintela, M. A. *Langmuir* **2008**, *24*, 12690.
(30) Pyykkö, P. *Chem. Soc. Rev.* **2008**, *37*, 1967.
(31) Coquet, R.; Howard, K. L.; Willock, D. J. *Chem. Soc. Rev.* **2008**, *37*, 2046.
(32) Häkkinen, H. *Chem. Soc. Rev.* **2008**, *37*, 2046.
(33) Hvolbæk, B.; Janssens, T. V. W.; Clausen, B. S.; Falsig, H.; Christensen, C. H.; Nørskov, J. K. *Nano Today* **2007**, *2*, 14.
(34) Johnson, G. E.; Mitrić, R.; Bonacić-Koutecký, V.; Castleman, A. W., Jr. *Chem. Phys. Lett.* **2009**, *475*, 1.
(35) Sanchez, A.; Abbet, S.; Heiz, U.; Schneider, W.-D.; Hakkinen, H.; Barnett, R. N.; Landman, U. *J. Phys. Chem. A* **1999**, *103*, 9573.
(36) Landman, U.; Yoon, B.; Zhang, C.; Heiz, U.; Arenz, M. *Top. Catal.* **2007**, *44*, 145.
(37) Tsunoyama, H.; Ichikuni, N.; Sakurai, H.; Tsukuda, T. *J. Am. Chem. Soc.* **2009**, *131*, 7086.
(38) Joshi, A. M.; Delgass, W. N.; Thomson, K. T. *J. Phys. Chem. B* **2006**, *110*, 23373.
(39) Hughes, M. D.; Xu, Y.-J.; Jenkins, P.; McMorn, P.; Landon, P.; Enache, D. I.; Carley, A. F.; Attard, G. A.; Hutchings, G. J.; King, F.; Stitt, E. H.; Johnston, P.; Griffin, K.; Kiely, C. J. *Nature* **2005**, *437*, 1132.
(40) Landon, P.; Collier, P. J.; Papworth, A. J.; Kiely, C. J.; Hutchings, G. J. *Chem. Commun.* **2002**, 2058.
(41) Cherétien, S.; Gordon, M. S.; Metiu, H. *J. Chem. Phys.* **2004**, *121*, 3756.
(42) Cherétien, S.; Gordon, M. S.; Metiu, H. *J. Chem. Phys.* **2004**, *121*, 9931.
(43) Lee, S.; Molina, L. M.; López, M. J.; Alonso, J. A.; Hammer, B.; Lee, B.; Seifert, S.; Winans, R. E.; Elam, J. W.; Pellin, M. J.; Vajda, S. *Angew. Chem., Int. Ed.* **2009**, *48*, 1467.
(44) Lyalin, A.; Taketsugu, T. *J. Phys. Chem. C* **2009**, *113*, 12930.
(45) Kang, G.-J.; Chen, Z.-X.; Li, Z. *J. Chem. Phys.* **2009**, *131*, 034710.
(46) Burke, K.; Perdew, J. P.; Wang, Y. In *Electronic Density Functional Theory: Recent Progress and New Directions*; Dobson, J. F., Vignale, G., Das, M. P., Eds.; Plenum Press: New York, 1998.
(47) Huber, K. P.; Herzberg, G. *Molecular Spectra and Molecular Structure*; Van Nostrand Reinhold: New York, 1979.
(48) Carter, E. A.; Goddard, W. A., III *J. Chem. Phys.* **1988**, *88*, 3132.
(49) Hay, P. J.; Wadt, W. R. *J. Chem. Phys.* **1985**, *82*, 299.
(50) Dunning, T. H., Jr. *J. Chem. Phys.* **1989**, *90*, 1007.
(51) Frisch, M. J.; Trucks, G. W.; Schlegel, H. B.; Scuseria, G. E.; Robb, M. A.; Cheeseman, J. R.; Montgomery, J. A., Jr.; Vreven, T.; Kudin, K. N.; Burant, J. C.; Millam, J. M.; Iyengar, S. S.; Tomasi, J.; Barone, V.; Mennucci, B.; Cossi, M.; Scalmani, G.; Rega, N.; Petersson, G. A.; Nakatsuji, H.; Hada, M.; Ehara, M.; Toyota, K.; Fukuda, R.; Hasegawa, J.; Ishida, M.; Nakajima, T.; Honda, Y.; Kitao, O.; Nakai, H.; Klene, M.; Li, X.; Knox, J. E.; Hratchian, H. P.; Cross, J. B.; Bakken, V.; Adamo, C.; Jaramillo, J.; Gomperts, R.; Stratmann, R. E.; Yazyev, O.; Austin, A. J.; Cammi, R.; Pomelli, C.; Ochterski, J. W.; Ayala, P. Y.; Morokuma, K.; Voth, G. A.; Salvador, P.; Dannenberg, J. J.; Zakrzewski, V. G.; Dapprich, S.; Daniels, A. D.; Strain, M. C.; Farkas, O.; Malick, D. K.; Rabuck, A. D.; Raghavachari, K.; Foresman, J. B.; Ortiz, J. V.; Cui, Q.; Baboul, A. G.; Clifford, S.; Cioslowski, J.; Stefanov, B. B.; Liu, G.; Liashenko, A.; Piskorz, P.; Komaromi, I.; Martin, R. L.; Fox, D. J.; Keith, T.; Al-Laham, M. A.; Peng, C. Y.; Nanayakkara, A.; Challacombe, M.; Gill, P. M. W.; Johnson, B.; Chen, W.; Wong, M. W.; Gonzalez, C.; Pople, J. A. *Gaussian 03*, revision C.02; Gaussian, Inc.: Wallingford, CT, 2004.
(52) Solov'yov, I. A.; Solov'yov, A. V.; Greiner, W.; Koshelev, A.; Shutovich, A. *Phys. Rev. Lett.* **2003**, *90*, 053401.

(53) Goldberg, D. E. *Genetic Algorithms in Search, Optimization, and Machine Learning*; Addison-Wesley Publishing Co.: Reading, MA, 1989.
(54) Michalewicz, Z. *Genetic Algorithms + Data Structures = Evolution Programs*, 3rd ed.; Springer-Verlag: Berlin, Germany, 1996.
(55) Ohno, K.; Maeda, S. *Chem. Phys. Lett.* **2004**, *384*, 277.
(56) Maeda, S.; Ohno, K. *J. Phys. Chem. A* **2005**, *109*, 5742.
(57) Ohno, K.; Maeda, S. *J. Phys. Chem. A* **2006**, *110*, 8933.
(58) Lyalin, A.; Solov'yov, I. A.; Solov'yov, A. V.; Greiner, W. *Phys. Rev. A* **2003**, *67*, 063203.
(59) Lyalin, A.; Solov'yov, A. V.; Greiner, W. *Phys. Rev. A* **2006**, *74*, 043201.
(60) Lyalin, A.; Solov'yov, I. A.; Solov'yov, A. V.; Greiner, W. *Phys. Rev. A* **2007**, *75*, 053201.
(61) Ding, X.; Li, Z.; Yang, J.; Hou, J. G.; Zhu, Q. *J. Chem. Phys.* **2004**, *120*, 9594.
(62) Fernández, E. M.; Soler, J. M.; Garzón, I. L.; Balbás, L. C. *Phys. Rev. B* **2004**, *70*, 165403.
(63) Walker, A. W. *J. Chem. Phys.* **2005**, *122*, 094310.
(64) Xiao, L.; Tollberg, B.; Hu, X.; Wang, L. *J. Chem. Phys.* **2006**, *124*, 114309.
(65) Häkkinen, H.; Yoon, B.; Landman, U.; Li, X.; Zhai, H.; Wang, L. *J. Phys. Chem. A* **2003**, *107*, 6168.
(66) McKenna, K. P.; Shluger, A. L. J. *J. Phys. Chem. C* **2007**, *111*, 18848.
(67) Rioux, R. M.; Hoefelmeyer, J. D.; Grass, M.; Song, H.; Niesz, K.; Yang, P.; Somorjai, G. A. *Langmuir* **2008**, *24*, 198.
(68) Harding, C.; Habibpour, V.; Kunz, S.; Nam-Su Farnbacher, A.; Heiz, U.; Yoon, B.; Landman, U. *J. Am. Chem. Soc.* **2009**, *131*, 538.
(69) Reed, A. E.; Curtiss, L. A.; Weinhold, F. *Chem. Rev.* **1988**, *88*, 899.
(70) Fernández, E. M.; Ordejón, P.; Balbás, L. C. *Chem. Phys. Lett.* **2005**, *408*, 252.
(71) Ekardt, W. *Phys. Rev.* **1984**, *29*, 1558.
(72) Knight, W. D.; Clemenger, K.; de Heer, W. A.; Saunders, W. A.; Chou, M. Y.; Cohen, M. L. *Phys. Rev. Lett.* **1984**, *52*, 2141.
(73) Castleman, A. W., Jr.; Khanna, S. N. *J. Phys. Chem. C* **2009**, *113*, 2664.
(74) Matveentzev, A.; Lyalin, A. G.; Solov'yov, I. A.; Solov'yov, A. V.; Greiner, W. *Int. J. Mod. Phys. E* **2003**, *12*, 81.
(75) Lee, T. H.; Ervin, K. M. *J. Phys. Chem.* **1994**, *98*, 10023.
(76) Wu, X.; Senapati, L.; Nayak, S. K.; Selloni, A.; Hajaligol, M. *J. Chem. Phys.* **2002**, *117*, 4010.
(77) Shimanouchi, T. Tables of Molecular Vibrational Frequencies Consolidated; National Bureau of Standards: Washington, DC, 1972; Vol. 1, pp 1−160.
(78) Yagi, K.; Hirao, K.; Taketsugu, T.; Schmidt, M. W.; Gordon, M. S. *J. Chem. Phys.* **2004**, *121*, 1383.

JP909505Y